corner of its assigned air space. It is likely that a human pilot would develop a similar behavior.

Conclusion

The implementation of pilot behavior with a parameterized set of rules is seen to be an effective way to represent a vast array of alternative behaviors. It can easily be set to mimic the behavior of human operators over a limited domain. In addition, any knowledge obtained during the evolutionary adaptation can be readily extracted from the new control parameter values. The genetic algorithm is seen to be an effective method for evolving a population of trial control parameters in a continuous search for better-adapted behaviors in a complex, dynamic environment. The use of an internal simulation is seen to be a practical way to represent knowledge about the external world.

The adaptive pilot model was able to generate behaviors that were significantly better than those of preprogrammed models. Like the human pilot it emulates, the pilot model can adapt its behavior when faced with novel threats and, thus, significantly reduce the fraction of missiles that leak through.

References

[1]Danczyk, G., Mortenson, S., Sailor, W., and Stroud, P., "Airplane Based Free Electron Laser Concept Overview," *PBFEL Workshop Proceedings*, edited by S. Singer, Los Alamos National Lab., Los Alamos, NM, 1990.

[2]Forden, G. E., "The Airborne Laser," *IEEE Spectrum*, Vol. 34, No. 9, 1997, pp. 40–49.

[3]Stroud, P. D., "Anisoplanatism in Adaptive Optics Compensation of a Focused Beam with Use of Distributed Beacons," *Journal of the Optical Society of America A*, Vol. 13, No. 4, 1996, pp. 868–874.

[4]Stroud, P. D., "Learning and Adaptation in an Airborne Laser Fire Controller," *IEEE Transactions on Neural Networks*, Vol. 8, No. 5, 1997, pp. 1078–1089.

[5]Holland, J. H., *Adaptation in Natural and Artificial Systems*, MIT Press, Cambridge, MA, 1992, p. 28.

Chaos in Wraparound Fin Projectile Motion

W. Asrar,* M. F. Baig,† and S. A. Khan*
Aligarh Muslim University, Aligarh 202002, India

Nomenclature

C_d	= coefficient of drag
C_l	= rolling moment coefficient
C_N	= normal force coefficient
C_n	= yawing moment coefficient
C_y	= lateral force coefficient
d	= body diameter, reference length
I_{xx}, I_{yy}, I_{zz}	= moments of inertia
I_{xy}, I_{xz}, I_{yz}	= products of inertia
l, m, n	= x, y, z components of aerodynamic moments
M	= Mach number
p, q, r	= roll, pitch, and yaw rates
Q	= dynamic pressure
S	= reference area, $\pi d^2/4$
T_x, T_y, T_z	= thrusts in x, y, and z directions
T^2	= torus with two frequencies
T^3	= torus with three frequencies
t	= time
V	= translational velocity
W_0	= total mass
α, β, Ψ	= angles of attack, side slip, and yaw
δ	= fin cant angle
δ_1, δ_2	= thrust misalignment angles
θ, ϕ, φ	= rotation angles
ω_p	= pitch frequency

Received Jan. 9, 1996; presented as Paper 96-0066 at the 34th Aerospace Sciences Meeting, Reno, NV, Jan. 15–19, 1996; revision received Oct. 17, 1997; accepted for publication Oct. 22, 1997.

*Reader, Department of Mechanical Engineering.

†Lecturer, Department of Mechanical Engineering. E-mail: met44mfb@amu.nic.in. Member AIAA.

Introduction

PROJECTILES with wraparound fins (WAF) have acute inherent dynamic instability. They show unfavorable damping characteristics, which lead to unpredictable flight behavior in pitch and yaw rates as well as in angle of attack and sideslip angle. Through the concept of a slightly asymmetric missile, Nicolaides[1] showed the possibility of roll resonance. Nicolaides[2] further put forward the idea of roll lock-in and catastrophic yaw. A more general analysis of the motion of rolling asymmetric bodies was presented by Murphy.[3] Nayfeh and Saric[4] analyzed the roll resonance of a re-entry vehicle and obtained necessary conditions for roll lock-in to occur. A more detailed work on roll lock-in of finned projectiles was done by Murphy.[5] Ananthkrishnan and Raisinghani[6] explored the stability of lock-in solutions and roll resonance.

A numerical study of nonlinear dynamics of WAF projectiles from the viewpoint of chaos is presented here. The aims of the study are to find the boundaries of periodic, quasiperiodic, and chaotic motions; to ascertain whether roll–pitch resonance lock-in occurs through phase portrait analysis; and to activate roll breakout by controlling the rotation number.

The scope of the work can be seen from two viewpoints: either elimination of chaos during the design phase of WAF projectiles or inclusion of controlled chaos to make the space–time trajectory unpredictable.

Mathematical Model

The equations of motion are derived with respect to a fixed-plane coordinate system. The x-axis points downrange, the y-axis points to the left looking downrange, and the z-axis points up:

$$\frac{\mathrm{d}p}{\mathrm{d}t} = \big[QSdC_l + qr(I_{yy} - I_{zz}) + (q^2 - r^2)I_{yz} + pqI_{zx} - prI_{xy} + qI_{xy} + rI_{zx}\big]\big/I_{xx} + (-pI_{xx} + qI_{xy} + rI_{xz})/I_{xx} \tag{1}$$

$$\frac{\mathrm{d}q}{\mathrm{d}t} = \big[QSdC_m + rp(I_{zz} - I_{xx}) + (r^2 - p^2)I_{zx} + qrI_{xy} - pqI_{yz} - pI_{xy} + rI_{yz}\big]\big/I_{yy} \tag{2}$$

$$\frac{\mathrm{d}r}{\mathrm{d}t} = \big[QSdC_n + pq(I_{xx} - I_{yy}) + (p^2 - q^2)I_{zx} + qrI_{xy} - qrI_{zx} + pI_{zx} + qI_{yz}\big]\big/I_{zz} \tag{3}$$

$$\frac{\mathrm{d}V}{\mathrm{d}t} = -\frac{QSC_{d\text{wind}}}{W_0} + g\cos\phi(\cos\theta\sin\alpha\cos\beta + \sin\phi\cos\theta\sin\beta - \sin\theta\cos\phi\cos\beta) + \frac{T_x}{W_0}\cos\alpha\cos\beta + \frac{T_y\sin\beta + T_z\sin\alpha\cos\beta}{W_0} \tag{4}$$

$$\frac{\mathrm{d}\alpha}{\mathrm{d}t} = -\frac{QSC_l}{W_0V\cos\beta} + q - \tan\beta(p\cos\alpha + r\sin\alpha) + \frac{g}{V\cos\beta} + (\cos\phi\cos\theta\cos\alpha + \sin\theta\sin\alpha) - \frac{T_x\sin\alpha - T_z\cos\alpha}{W_0V\cos\beta} \tag{5}$$

$$\frac{d\beta}{dt} = \frac{QSC_{ywind}}{W_0 V} + p\sin\alpha - r\cos\alpha + \frac{g}{V}\cos\beta\sin\phi\cos\theta + \frac{\sin\beta}{V}(g\cos\alpha\sin\theta - g\sin\alpha\cos\phi\cos\theta) + \frac{-T_x\cos\alpha - T_z\sin\alpha}{W_0 V} + \frac{T_y\cos\beta}{W_0 V} \tag{6}$$

Because attitude–position measurements are made with respect to an Earth-fixed axis system, additional transformation equations are shown next in terms of the fixed-plane Euler angles θ and φ and angle of rotation ϕ:

$$\frac{d\theta}{dt} = q\cos\phi - r\sin\phi \tag{7}$$

$$\frac{d\varphi}{dt} = \frac{r\cos\phi + q\sin\phi}{\cos\theta} \tag{8}$$

$$\frac{d\phi}{dt} = p + r\tan\theta\cos\phi + q\sin\phi\tan\theta \tag{9}$$

The aerodynamic force and moment coefficients expressed by C_N, C_y, C_n, C_l, etc., follow the standard definitions, as given in Ref. 7.

Equations (1–9) are solved numerically using a Runge–Kutta–Fehlberg scheme for various values of the fin canting angle δ. This has been included in the code by variation of aerodynamic coefficients and derivatives such as $C_{lp}, C_{mq}, C_{n\alpha}, C_d$, CP_{tail}, CP_{nose}, etc., with Mach number (0.1–2.5) for different canting angles (−3–3 deg).

Analysis

Analyses of the dynamic variables have been performed using a time history of signals, phase portraits, Poincaré sections, power spectrum estimation, and autocorrelation. The variation in canting angle brings about small but consequential changes in the dynamics of pitching and yawing angular velocities, angle of attack, and side slip angle, whereas the rest of the dynamic variables exhibit steady-state motion.

For these four dynamic variables, the time history of the signals at various canting angles shows a change from periodic to low-frequency quasiperiodic to multiple-frequency quasiperiodic motion and then back to low-frequency quasiperiodic to periodic motion as the magnitude of canting is increased from 0.0 to 3.0 (or decreased to −3.0) deg. The phenomenon of roll–pitch resonance can be seen by analyzing the phase portrait and Poincaré sections of either yaw or pitch angular velocities or of angle of attack. The roll breakout can be activated by crossing the critical rotation number (p/ω_p) of 3. Moreover, other dynamically unstable problems such as the occurrence of catastrophic yaw can be investigated from power spectrum, time history, and correlation signals.

The canting of the fins is done both clockwise and counterclockwise, i.e., positive and negative angles, and it is observed that at zero cant the missile exhibits steady-state nonoscillatory motion for all of the dynamic variables. A further increase in the range 0.05–0.2 deg results in observance of periodic motion in four dynamic variables (q, r, α, and β).

For the canting angle regime of 0.2–0.6 deg, quasiperiodic motion is observed. From 0.6- to 1.8-deg fin canting, roll lock-in occurs, which results in multiple-frequency quasiperiodic motion (Fig. 1) of all four dynamic variables mentioned. A low-dimensional strange attractor is observed at $\delta = 1.0$. Increasing δ from 1.8 to 2.7 deg results in the gradual disappearance of the strange attractor and formation of a T^2 torus at 1.9 deg. This roll breakout is observed at the critical rotation number value of 3. After the roll breakout the dynamic system reverts back to quasiperiodic motion. From 2.7- to 3.0-deg fin canting, the T^2 torus disappears, and the system reverts to the periodic regime.

There is a gradual shift of power-dominant frequencies to higher values as the δ is increased from 0.0 to 1.8 deg. Moreover, the power contained in the subharmonic frequencies for multiple-frequency quasiperiodic motion is approximately 10 times greater than that

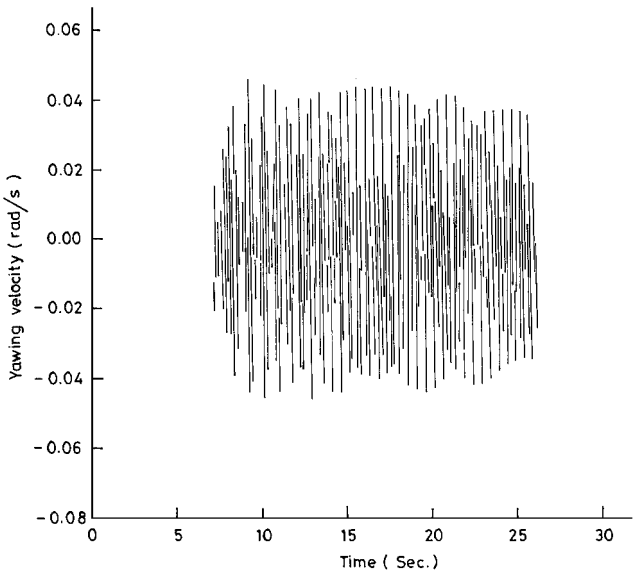

Fig. 1 Yawing velocity vs time for weak chaotic motion at fin cant = 1.0 deg.

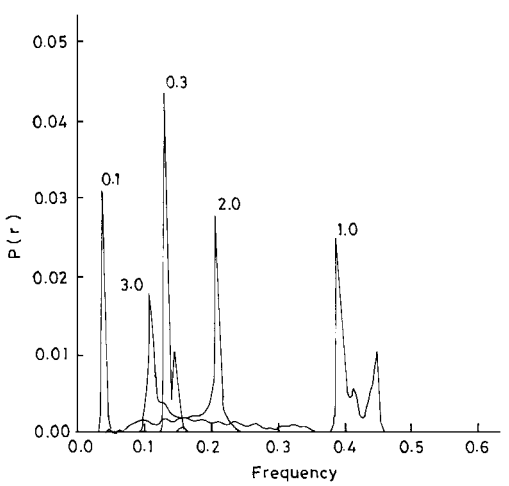

Fig. 2 Power spectrum of pitching velocity showing frequency shift at various canting angles.

for subharmonics in the quasiperiodic regime. This aspect of power concentration is in contrast to the aspect of power spread as occurs in chaos in fluid flows.[8] For $\delta \geq 1.8$, the power-dominant frequencies again start shifting to lower values, with a consequent increase in the magnitude of power (Fig. 2).

The autocorrelation of any one of the four dynamic signals exhibits a gradual decrease in amplitude from periodic to quasiperiodic to weak chaotic motion as δ is increased. To check the consistency of the critical value of the rotation number, the inertia of the projectile was increased to reduce ω_p by 25%; nonetheless, the critical rotation number remained invariably constant.

Conclusion

The following conclusions have been reached.

1) The dynamic variables such as pitching angular velocity, yawing angular velocity, angle of attack, and sideslip angle all show multiple quasiperiodicity as the fin canting angle δ is varied.

2) Periodic motions are observed for pitching and yawing angular velocities, angle of attack, and sideslip angles for canting angles in the range 0.05–0.2 deg.

3) Low-frequency quasiperiodic motion is observed for the same dynamic variables just mentioned for canting angles in the range 0.2–0.6 deg. The formation of degree two and three toruses is observed as δ is varied.

4) Roll breakout can be achieved by crossing the 3:1 critical ratio of roll–pitch angular velocities.

5) Further increase of canting angle 1.9–2.7 deg results in quasi-periodic motion.

6) From 2.7 to 3.0 deg periodicity again appears.

References

[1]Nicolaides, J. D., "On the Free Flight Motion of Missiles Having Slight Configurational Asymmetries," U.S. Army Ballistics Research Lab., Rept. R858, Aberdeen Proving Ground, MD, June 1953.

[2]Nicolaides, J. D., "Two Nonlinear Problems in the Flight Mechanics of Modern Ballistic Missiles," Inst. of Aeronautical Sciences, Rept. 59-11, Univ. of Toronto, ON, Canada, Jan. 1959.

[3]Murphy, C. H., "Responses of an Asymmetric Missile to Spin Varying Through Resonance," *AIAA Journal*, Vol. 9, No. 11, 1971, pp. 2197–2201.

[4]Nayfeh, A. H., and Saric, W. S., "An Analysis of Asymmetric Rolling Bodies with Nonlinear Aerodynamics," *AIAA Journal*, Vol. 10, No. 8, 1972, pp. 1004–1011.

[5]Murphy, C. H., "Some Special Cases of Spin-Yaw Lock In," *Journal of Guidance, Control, and Dynamics*, Vol. 12, No. 6, 1989, pp. 771–776.

[6]Ananthkrishnan, N., and Raisinghani, S. C., "Steady and Quasisteady Resonant Lock-In of Finned Projectiles," *Journal of Spacecraft and Rockets*, Vol. 29, No. 5, 1992, pp. 692–696.

[7]Ashley, H., *Engineering Analysis of Flight Vehicles*, Addison-Wesley, Reading, MA, 1974, pp. 173–202.

[8]Gollub, J. P., and Swinney, H. L., "Onset of Turbulence in a Rotating Fluid," *Physical Review Letters*, Vol. 35, Dec. 1975, pp. 927–930.

Decentralized Control of Expandingly Constructed Large Space Structures

Takashi Kida*
University of Electro-Communications, Tokyo 182, Japan
and
Keiji Komatsu† and Isao Yamaguchi‡
National Aerospace Laboratory, Tokyo 182, Japan

Introduction

IT is likely that future large space structures will be constructed by docking several modules together in orbit. Before docking, each module is stabilized by its own controller. However, the stability of the connected system is not guaranteed by the local controllers because they are designed for the isolated subsystems. In view of this, there is a need to design a stabilizing controller for the docking case when the plant properties drastically change. Decentralized control technology, which has the potential capability to stabilize interconnected systems with information constraints, seems to meet this requirement. A great deal of research has been carried out on this problem.[1–5] Their common framework is to obtain decentralized control system stability under the structural perturbations that result when modules are connected and disconnected in arbitrary ways. By this method, a set of local controllers achieves connective stability for space structures of arbitrary configuration. However, this is not necessarily the case in an actual construction scenario. It is usual that space structures are constructed by connecting new modules to already existing structures one after another. In this case, only the local controller of the new module should be designed so as to stabilize the connected system, without changing the existing system. This is called the expanding system problem.[6–8] This Note investigates stabilization during this type of construction. The controller design procedure is formulated in a μ synthesis framework, and a simple numerical example is used to illustrate its capability.

Received May 1, 1997; revision received Nov. 7, 1997; accepted for publication Nov. 26, 1997.

*Professor, Department of Mechanical and Control Engineering, Chofugaoka 1-5-1, Chofu. Senior Member AIAA.

†Senior Researcher, Structural Dynamics Division, Jindaiji-Higashi 7-44-1, Chofu. Member AIAA.

‡Senior Researcher, Control Technology Division, Jindaiji-Higashi 7-44-1, Chofu. Member AIAA.

Problem Definition

Consider a space structure $\mathcal{S}$ to be constructed in orbit by connecting two modules $\mathcal{S}_1$ and $\mathcal{S}_2$. The mathematical models of $\mathcal{S}_i$ $(i = 1, 2)$ are described by modal equations:

$$M_i \ddot{p}_i + D_i \dot{p}_i + K_i p_i = L_i u_i, \qquad y_i = H_i p_i \tag{1}$$

where $p_i \in R^{N_i}$ is the modal coordinate vector and u_i and y_i are the control input and measurement output vectors, respectively. The diagonal matrices M_i, D_i, and K_i are the mass, damping, and stiffness in modal space. The connected system $\mathcal{S}$ after docking can be modeled by a direct finite element method (FEM) analysis or by a component mode synthesis.[9] Regardless of the approach taken, however, it is ultimately described by another modal equation as follows:

$$\begin{aligned} M\ddot{p} + D\dot{p} + Kp &= L_{\cdot 1}u_1 + L_{\cdot 2}u_2 \\ y_1 = H_{1\cdot}p, &\qquad y_2 = H_{2\cdot}p \end{aligned} \tag{2}$$

where $p \in R^N$ is the global modal coordinate after docking. The purpose of decentralized control synthesis is to obtain a pair of controllers

$$u_i = C_i(s)y_i \tag{3}$$

for $i = 1, 2$, which stabilizes $\mathcal{S}_1$, $\mathcal{S}_2$, and $\mathcal{S}$. We design the controllers by the following two steps: 1) design $C_1(s)$, which stabilizes $\mathcal{S}_1$, and 2) design $C_2(s)$, which stabilizes $\mathcal{S}_2$ and $\hat{\mathcal{S}}$ simultaneously, where $\hat{\mathcal{S}}$ is the closed-loop system of $\mathcal{S}$ with the controller $u_1 = C_1(s)y_1$. Because the first step is the ordinary vibration control problem, it will not be discussed in detail here. The design problem of $C_2(s)$ is investigated in the next section.

Controller Synthesis

We first derive two conditions for $C_2(s)$ to stabilize $\mathcal{S}_2$ and $\hat{\mathcal{S}}$ independently. It will then be shown that the latter condition includes the former under an assumption. The controller must be a reduced-order controller because the model order of Eqs. (1) and (2) is excessively large. This is an essential requirement for a vibration control problem. To investigate the controller stabilizing $\mathcal{S}_2$, Eq. (1) is rewritten in the frequency domain as $y_2 = P_2(s)u_2$. Then we separate $P_2(s)$ into a control model $Q_2(s)$ and a residual model $R_2(s)$ as $P_2(s) = Q_2(s) + R_2(s)$. We regard $Q_2(s)$ as the nominal model whose state-space realization is $Q_2(s) = C(sI - A)^{-1}B$, where $A \in R^{2n_2 \times 2n_2}$ and $n_2 \ll N_2$. Then $\mathcal{S}_2$ is equivalent to an extended system:

$$y_2 = Q_2(s)u_2 + w_2, \qquad z_2 = u_2$$

having the model error loop $w_2 = R_2(s)z_2$. Therefore, if $C_2(s)$ stabilizes $Q_2(s)$ and satisfies

$$\|R_2T\|_\infty < 1, \qquad T(s) = C_2(s)[I - Q_2(s)C_2(s)]^{-1} \tag{4}$$

then $\mathcal{S}_2$ is robustly stabilized against $R_2(s)$. Next, the condition under which $C_2(s)$ stabilizes $\hat{\mathcal{S}}$ is considered. From Eq. (2), $\mathcal{S}$ is

$$y_1 = P_{11}(s)u_1 + P_{12}(s)u_2, \qquad y_2 = P_{21}(s)u_1 + P_{22}(s)u_2$$

in the frequency domain. Then the closed-loop system $\hat{\mathcal{S}}$ produced by $C_1(s)$ becomes

$$y_2 = \hat{P}_2(s)u_2, \qquad \hat{P}_2 = P_{21}C_1(I - P_{11}C_1)^{-1}P_{12} + P_{22} \tag{5}$$

We again describe $P_{ij}(s) = Q_{ij}(s) + R_{ij}(s)$ for $i, j = 1, 2$ so that $Q_{ij}(s)$ has the same number of modes as $Q_2(s)$; i.e., its realization is $Q_{ij}(s) = C_{q_i}(sI - A_q)^{-1}B_{q_j}$, where $A_q \in R^{2n_2 \times 2n_2}$. In the sequel,